0.8-eV photoluminescence of GaAs grown by molecular-beam epitaxy at low temperatures

P. W. Yu and G. D. Robinson
University Research Center, Wright State University, Dayton, Ohio 45435

J. R. Sizelove and C. E. Stutz
Solid State Electronics Directorate, Wright Laboratory (WL/ELR), Wright-Patterson Air Force Base, Ohio 45433
(Received 14 May 1993; revised manuscript received 28 June 1993)

We report deep-center photoluminescence of GaAs grown at low temperatures between 200 and 400 °C by molecular-beam epitaxy. Changes of temperature and excitation intensity were used in addition to heat-treatment and photoluminescence-excitation measurements. The type of photoluminescence transition strongly depends on the growth temperature and the $[As_4]/[Ga]$ ratio. The layers grown at 200–300 °C show a dominant emission at 0.68 eV ($EL2$) and an emission at 1.1 eV related to a V_{Ga} center. The layers grown at 325–400 °C show one transition at 0.75–0.81 eV (designated as the 0.8-eV emission). We attribute the 0.8-eV emission to the As_i-V_{Ga} center. The center shows the large lattice relaxation exemplified by the Franck-Condon shift of 0.34 eV. The thermal ionization energy is determined to be 0.36 eV. We discuss our assignment of the As_i-V_{Ga} center to the well-known $EL6$ center.

I. INTRODUCTION

Single-crystal GaAs grown by molecular-beam epitaxy (MBE) at the low temperatures of 200–400 °C is a unique material that has generated great technological and scientific interest over the last few years. Low-temperature GaAs buffer layers can prevent[1] sidegating or backgating effects in metal-semiconductor field-effect transistors by providing excellent device isolation. Low-temperature GaAs used as an active layer supports the construction of photodetectors, with time constants in the femtosecond range.[2] In order to obtain a better understanding of the electrical and optical properties of low-temperature GaAs we must understand how As is incorporated into the material.

Particle-induced x-ray emission analysis using a H^+ beam showed[3] low-temperature GaAs to have ~ 1 at. % excess As in the material grown at 200 °C. The excess As is incorporated[3] as $\sim 10^{20}$ cm^{-3} As-antisite-related centers in as-grown materials and as As precipitates in annealed materials.[4] Annealing at 600 °C also changes the layer conductivity from a low-resistivity state to a high-resistivity state.[5] The conduction mechanism of low-temperature GaAs is presently explained by two models based on the defect-band hopping[6] and As precipitate.[5] The conduction mechanism is primarily influenced by intrinsic defects such as the antisite defect (As_{Ga}), gallium vacancy (V_{Ga}), arsenic interstitial (As_i), and associated pair defects. Deep-level emission originating from the defects can be expected to dominate the radiative mechanism of low-temperature GaAs. Viturro, Melloch, and Woodall[7] observed a cathodoluminescence emission at ~ 1 eV from a 250 °C grown material and assigned it to a transition involving $EL2$ and the valence band. Also, Ohbu, Takahama, and Kimura[8] observed a photoluminescence (PL) emission at 1.24 eV from a 300 °C grown and 800 °C annealed material which was assigned to a transition involving V_{Ga}.

We report here a PL emission band at ~ 0.8 eV which dominates the deep-center radiative mechanism for low-temperature MBE GaAs grown at temperatures between 325 and 400 °C. We measured excitation intensity and temperature dependence of the PL and photoluminescence-excitation (PLE) spectra. Heat treatments were also made at temperatures of 200–700 °C. The heat-treatment behavior of the sharp exciton line[9,10] at 1.467 eV is compared to that of the 0.8-eV emission. The comparison allows us to identify the center responsible for the 0.8-eV emission as an $(As_i - V_{Ga})C_{3v}$-type defect. Other experimental evidence to support this assignment are presented.

II. EXPERIMENT

The MBE layers were grown in a Varian Gen-II system under As_4 using a nonindium bonded substrate holder. Growth temperatures were 200, 250, 270, 300, 325, 350, and 400 °C and were determined by a noncontacting thermocouple. A Perkin/Elmer arsenic cracker was used to produce As_4 with a constant cracker tube current of 2 A. This material was grown in the $[As_4]/[Ga]$ beam equivalent pressure (BEP) ratio range of 10–26. The 2-in. GaAs substrates used were of [100] orientation tilted 2° toward the nearest [110]. The substrates were etched and cleaned, loaded into the vacuum chamber, had the oxide thermally desorbed at 600 °C under arsenic overpressure, then the substrate temperature was reduced to the growth temperature also under arsenic overpressure. When 2 μm of low-temperature GaAs was grown, all samples had nice streaky reflection high-energy electron-diffraction patterns during the entire run.

PL measurements were made using a variable-temperature Janis optical dewar. The 5145 Å line of an Ar-ion laser was used as an excitation source with an intensity of 10^{-2}–10^{1} W/cm^2. PL spectra were obtained with Spex monochromators of focal length $f=0.5$ and

1.29 m and were detected with a C31034 photomultiplier tube, a liquid-nitrogen-cooled Ge and a liquid-nitrogen-cooled InAs detector. Standard synchronous techniques were used with a lock-in amplifier. PLE measurements were made with a Ti-Sapphire dye laser. Heat treatments were performed at 200–700 °C for 20 min in a furnace purged with flowing N_2. Another GaAs wafer was placed on top of the low-temperature layer during heat treatment in order to inhibit As loss.

PL efficiency is very low in low-temperature GaAs due to the abundance of nonradiative centers. Thus, PL generated from the semi-insulating GaAs bulk substrate often dominates the spectra. Our solution to this problem is to remove the substrate. An AlAs layer of 500-Å thick is inserted between the low-temperature GaAs layer and the substrate during MBE growth. Then, a 5×8-mm sample is cut from the wafer and epoxied, layer down, to a piece of microscope-slide glass. Next, the substrate, initially ~500 μm, is lapped to ~100 μm and polished to ~25 μm. After polishing, the rest of the substrate is removed by a reactive-ion etch, which stops on the AlAs, and finally, the AlAs is dissolved in HF acid. The finished samples are quite robust.

III. RESULTS AND DISCUSSION

Figure 1 shows 2-K PL spectra of 200, 250, 300, 325, and 400 °C grown layers. The 200 °C grown layers show two broad bands at approximately 0.68 and 1.1 eV, as shown in Fig. 1(a). The 0.68 and 1.1-eV bands are from wafers grown with the BEP ratio of 16 and 26, respectively. This indicates that the formation of deep centers strongly depends on the $[As_4]/[Ga]$ ratio. The 250° and 300 °C layers grown with the $[As_4]/[Ga]$ ratio of 15 show only one dominant PL band at 0.68 eV. However, with increasing growth temperature the 0.68- and 1.1-eV bands are quenched. New PL bands at 0.75 and 0.81 eV emerge, respectively, from 325 and 400 °C layers grown, respectively, with the $[As_4]/[Ga]$ ratio of 19 and 20. We designate the two peaks near 0.8 eV as "0.8-eV emission" considering the proximity of the peak position. Presently, we do not have a definite microscopic identification of the center responsible for the 1.1-eV emission. However, stoichiometry considerations and the instability of the emission lead to a V_{Ga}-related emission. The 0.68-eV emission can be attributed to the transition from the $EL2^0$ to the valence band based on the results of previous works.[11–13]

The 0.8-eV PL emission was first reported[14] in liquid encapsulated Czochralski (LEC) semi-insulating substrate GaAs and has been the subject of a number of subsequent PL investigations[15–20] for LEC substrate materials. The origin of the 0.8-eV emission has been suggested to be an association with "microdefects"[15] and the second level[16] of As_{Ga}. However, a consistent observation with respect to the 0.8-eV emission is that it has an M-shaped intensity profile across the diameter of a semi-insulating wafer, in contrast to the W-shaped profiles for the C_{As}-related 1.49-eV emission and the 0.68-eV $EL2$ emission. Recently, Shinohara[21] studied the 0.8-eV emission from the MBE GaAs layers grown at 550–730 °C and attributed

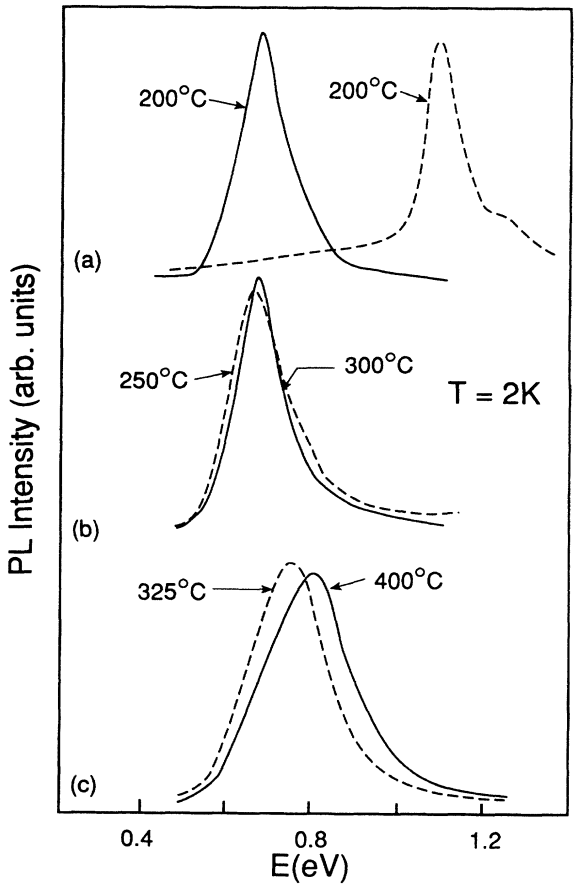

FIG. 1. Photoluminescence spectra from low-temperature GaAs grown at (a) 200 °C, (b) 250 and 300 °C, and (c) 325 and 400 °C.

the 0.8-eV emission to an As_{Ga}-V_{As} center.

Figure 2 shows the temperature dependence of the PL spectrum of the 0.8-eV emission in the temperature range of 30–150 K. The PL intensity and line shape do not change over the temperature range 2–50 K. However, for temperatures greater than 50 K, the PL intensity of the 0.8-eV emission decreased and the overall spectrum shows the presence of two overlapping components, the original 0.8-eV emission and the emerging 0.68-eV $EL2$ emission. The appearance of the 0.68-eV emission distorts the overall PL shape. With a further increase of temperature, the 0.68-eV emission dominates the overall PL shape as shown in Fig. 2(c). The dot-dashed and dashed curves in Fig. 2(b) and 2(c) are the extracted Gaussian-shaped spectra of the overlapping 0.68- and 0.8-eV emissions, respectively.

The half width at half maximum (W) of the 0.8-eV emission was obtained directly from the single 0.8-eV emission at $T<50$ K and from resolving the 0.68- and 0.8-eV emissions at $T\geq 50$ K. Known PL characteristics[11] of $EL2$ were used for the resolution: (i) the peak position of the 0.68-eV emission does not change at $T=4$–300 K; and (ii) the full width at half maximum of the 0.68-eV emission ($W_{0.68}$) is given by

$$W_{0.68}=[(8\ln 2)S(\hbar\omega)^2(2\bar{n}+1)]^{1/2}, \quad (1)$$

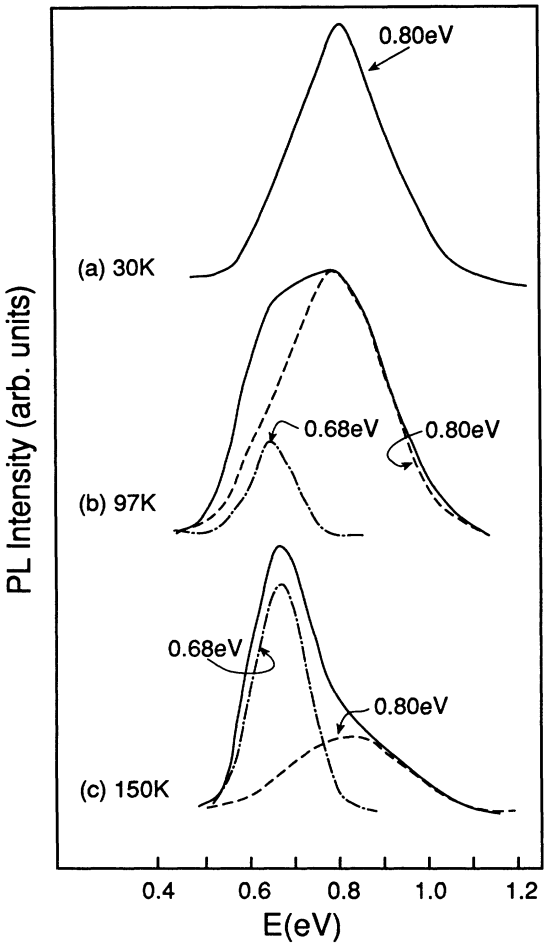

FIG. 2. Temperature-dependent characteristics of the 0.8-eV emission at 30–150 K. The dot-dashed and dashed curves in (b) and (c) are the spectra of the resolved 0.68-eV and 0.80-eV emissions, respectively.

where $\bar{n}=[\exp(\hbar\omega/kT)-1]^{-1}$, $\hbar\omega=20$ meV, and the Haung and Rhys constant $S=5.5$. The obtained half width at half maximum of the 0.8-eV emission ($W_{0.80}$) is shown in Fig. 3. The solid line is the fit of Eq. (1) to the experimental data with $\hbar\omega=38.7$ meV and $S=8.9$, which leads to the Franck-Condon shift $\Delta_{FC}=0.344$ eV. Then, the thermal ionization energy E_i for the center responsible for the 0.8-eV emission can be described by

$$E_i=E_g-h\nu_{LUM}-\Delta_{FC}\ , \tag{2}$$

where E_g is the band gap of GaAs and $h\nu_{LUM}$ is the transition energy of the 0.8-eV emission. From Eq. (2) we obtain $E_i=0.36$ eV using $E_g=1.519$ eV and $h\nu_{LUM}=0.81$ eV.

Figure 4 shows the PLE spectrum of the structure we have called the 0.8-eV emission for a sample with the peak at 0.81 eV. The low-energy threshold of the PLE spectrum is near 1.498 eV. The PLE threshold energy $h\nu_{PLE}$ is usually related to $h\nu_{LUM}$ by the following equation assuming the same configuration coordinate modes in the ground and excited states:

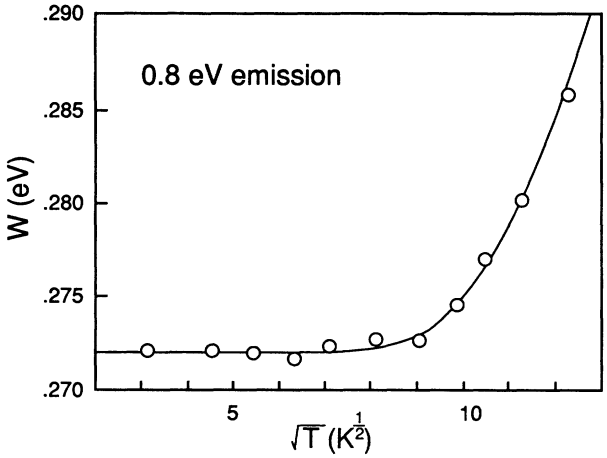

FIG. 3. The half width at half maximum (W) vs. $\sqrt{T}$ relation for the 0.80-eV emission.

$$h\nu_{PLE}=h\nu_{LUM}+2\Delta_{FC}\ . \tag{3}$$

The arrow in Fig. 4 shows the experimental $h\nu_{PLE}$ of 1.498 eV. The experimental PLE agrees very well with the calculated value of 1.49 eV. The difference of 8 meV can be ascribed to the different configuration coordinate modes in the ground and excited states.

Figure 5 shows PL spectra obtained for the 0.8-eV emission from an as-grown sample grown at 400 °C and from samples annealed at 393, 450, and 500 °C measured over the energy range 0.5–1.2 eV. The PL intensity of the 0.8-eV emission decreases with increasing annealing temperature for temperatures of 300–450 °C and the 0.68-eV emission appears with decreasing intensity of the 0.8-eV emission. After heat treating at 500 °C, the only radiative process is the 0.68-eV emission. With complete quenching of the 0.8-eV emission, the intensity of the 0.68-eV emission increases slightly. This can be explained by the dissociation of the center responsible for the 0.8-eV emission and by the transformation into another center. Figure 6 shows PL spectra in the energy

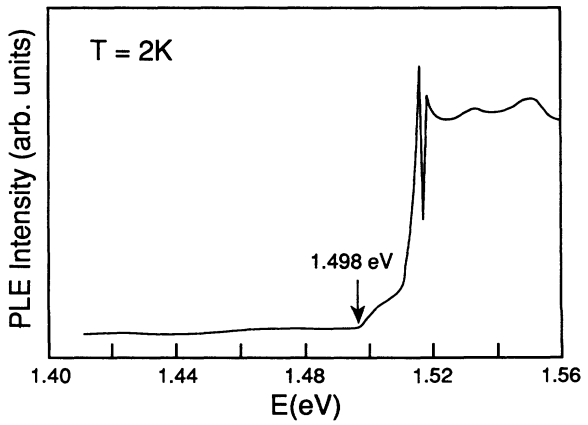

FIG. 4. Photoluminescence-excitation spectrum of the 0.8-eV emission. The energy of 1.498 eV is the calculated photoluminescence threshold energy.

range of 1.41–1.48 eV for the same samples used in Fig. 5. For the as-grown sample, the PL consists of no-phonon lines (1, 1′, 2, and 3) at ~1.47 eV and associated phonon sidebands of both lattice and localized vibrational modes of the C_{3v} symmetry As_i-V_{Ga} center as reported[9,10] earlier. Also, our recent numerical calculations[10] of localized vibrational modes for the As_i-V_{Ga} center clearly prove that the PL lines are indeed due to an exciton bound to that center. Effects of heat treatments, as seen in Figs. 6(b), 6(c), and 6(d), can be summarized as follows: (i) the gradual decrease of no-phonon line intensity with increasing annealing temperature, (ii) the gradual decrease and eventual disappearance of many lines between 1 and 14 with increasing annealing temperature, (iii) the strongly growing lines 9 and 14 with increasing annealing temperature, and (iv) the disappearance of all the sharp lines with 500 °C annealing. The details of the growing intensity of the lines 9 and 14 is not discussed here in detail. However, an important result of heat-treatment measurements is that the no-phonon lines due to the As_i-V_{Ga} center and the deep 0.8-eV emission show the same characteristics in terms of the annealing temperature: (i) for the heat treatments at 393 and 450 °C, gradual decrease of the no-phonon lines and the gradual shift of the peak position of the 0.8-eV emission to 0.68 eV with increasing heat-treatment temperature, and (ii) for 500- °C annealing, the complete disappearance of both the no-phonon lines and the 0.8-eV emission band. These experimental results are consistent with the 0.8-eV emission originating from the As_i-V_{Ga} center. The collapse of the As_i-V_{Ga} center contributes to additional As_{Ga} or As_i depending on the collapsing process. The As_i may cause the observed increases in the 9 and 14 sharp peaks. If we assume that the isolated As_{Ga} contributes to the increase in the 0.68 eV, $EL2$ center, we have two ways for the As_i-V_{Ga} center to evolve as follows:

$$(As_i - V_{Ga}) \rightarrow As_i + V_{Ga} , \tag{4a}$$

$$(As_i - V_{Ga}) \rightarrow As_{Ga} . \tag{4b}$$

The process (4a) is the dissociation of the pair whereas the process (4b) is the recombination mechanism by the hopping of the As_i into V_{Ga} to form As_{Ga}. In fact, the increased strength of lines 9 and 14 in Fig. 6 has been attributed to the increase of the As_{Ga}-C_{As} and As_{Ga}-As_i

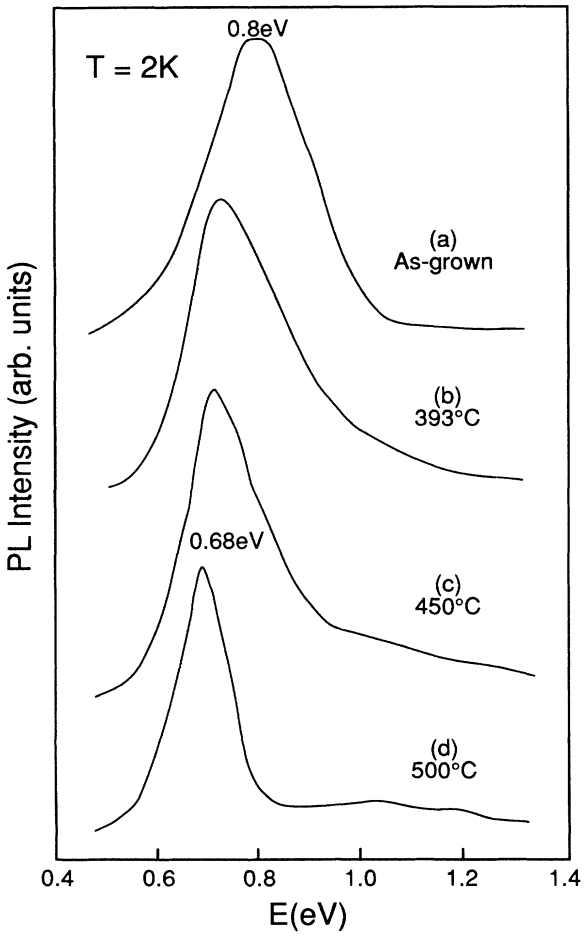

FIG. 5. 0.8-eV photoluminescence spectra obtained from (a) as-grown, (b) 393 °C annealed, (c) 450 °C annealed, and (d) 500 °C annealed samples. All samples were from one wafer grown at 400 °C.

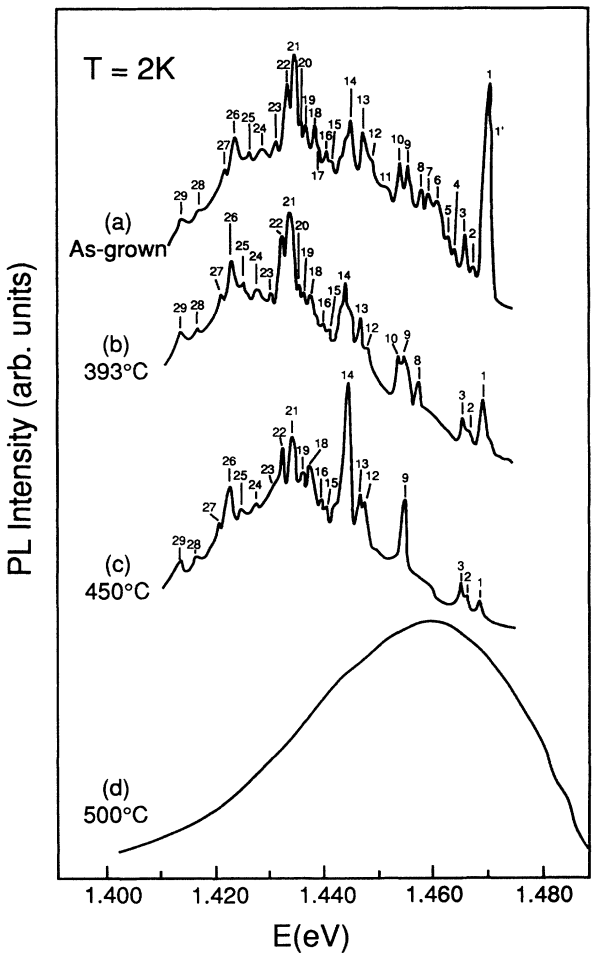

FIG. 6. Sharp-line emission spectra obtained from (a) as-grown, (b) 393 °C annealed, (c) 450 °C annealed, and (d) 500 °C annealed samples. All samples were from one wafer grown at 400 °C and are the same samples used for Fig.5

centers, respectively (the details were described in Ref. 10). The variation of PL excitation intensity with laser intensity in the range of 10^{-2}–10^{1} W/cm^2 did not change the peak position and line shape of the 0.8-eV emission. This indicates that the 0.8-eV emission is a transition from the As_i-V_{Ga} to the band edge.

The thermal ionization energy obtained from the Franck-Condon shift using Eq. (2) is 0.36 eV. However, it is not clear whether the level is from the conduction-band or valence-band edge. If the level captures electrons from the conduction band through the effective-mass shallow donor, the above-energy-gap PLE will show the oscillatory PLE structure due to the longitudinal optical-phonon emissions. In fact, such oscillatory PLE was observed[12] for 0.8-eV emission present in LEC semi-insulating GaAs and was explained by the electron capture into a deep donor level through the effective-mass shallow donor. Recently, we have performed a PLE experiment for the present low-temperature GaAs. We find the same above-gap oscillatory PLE[22] as found for LEC GaAs. Thus, the As_i-V_{Ga} is an electron trapping center and can be placed at $E_C-0.36$ eV. Then, the no-phonon lines (1, 1′, 2, and 3) at ~ 1.47 eV is due to the exciton bound to the 0.36-eV deep As_i-V_{Ga} center and due to the $1s$ state of the center. Resonant photoluminescence (RP) at the no-phonon lines was performed to find out the excited states such as the $2s$, $2p$, . . . of the center. We failed to observe the higher states. Earlier works[23,24] on high-purity excellent GaAs showed the presence of the two-electron and two-hole transitions, respectively, from the shallow effective-mass donor and C_{As} acceptor. However, the two-electron or two-hole transitions bound to a deep center was not observed. We attribute the failure of observing the excited states of the As_i-V_{Ga} center to the intrinsically poor material quality of the low-temperature GaAs.

Let us now consider the result of two previous works on $EL6$ and $EL2$ in neutron irradiated[25] and B-implanted[26] GaAs. The irradiation or implantation induced the formation of two donors, $EL6$ (E_c-0.35 eV) and $EL2$. An annealing study after the irradiation or implantation showed (i) that there is an interaction between $EL2$ and $EL6$ and (ii) that at the annealing temperatures of 400–600 °C, $EL6$ decreases by a pair-defect type dissociation whereas $EL2$ increases with increasing the heat-treatment temperature. These heat-treatment characteristics are almost the same as those of the 0.8-eV As_i-V_{Ga} and the 0.68 $EL2$ emission as discussed in connection with Fig. 5. Based on the almost identical value of thermal ionization of the As_i-V_{Ga} center and $EL6$, our recent PLE measurements, and the characteristics of $EL6$ and $EL2$ in the above experiments,[23,24] we tentatively attribute $EL6$ to the As_i-V_{Ga} center. By assuming that $EL2$ is the isolated[27] As_{Ga}, Eq. (4a) and (4b) can be described by the following processes:

$$EL6 \rightarrow As_i + V_{Ga} \ , \tag{5a}$$

$$EL6 \rightarrow EL2 \ . \tag{5b}$$

We think that the processes (5a) and (5b) can explain the results of the above heat-treatment experiment on $EL6$ and $EL2$. Thus, by assigning the As_i-V_{Ga} center to be a deep center at 0.36 eV from the conduction band, we construct the configuration coordinate model from the As_i-V_{Ga} center as shown in Fig. 7. The assignment of the (As_i-V_{Ga}) center to the 0.8-eV emission is also supported by the well-known W-shape and M-shape intensity profiles,[16,28,29] respectively, for the 0.68-eV $EL2$ and 0.8-eV V_{Ga}-As_i ($EL6$) centers. The PL intensities are influenced by the carrier concentration [n] and the trap concentration [N_T]. The carrier concentration is determined by the product of the carrier lifetime and carrier generation rate. The spectral distributions of carrier lifetime[30] and dislocation density[28] along the ⟨110⟩ direction across a LEC wafer show W shape in contrast to the M shape of the 0.8-eV emission. This indicates that the (V_{Ga}-As_i) increases in number causing the observed increase in PL intensity, that the concentration of $EL6$ is larger in the region where dislocation density is lower, and that dislocation produces $EL2$ in the region where dislocation density is higher. The production of $EL2$ by dislocation climb is well proven.[31,32] The assignment of the 0.8-eV emission to the (As_i-V_{Ga}) center clearly explains the W and M profiles in LEC GaAs.

Finally, we discuss other models for the 0.8-eV emission. "Microdefects"[15] were attributed to the 0.8-eV emission. However, it is difficult to clarify the microscopic picture of "microdefect." The second level of As_{Ga} was assigned[16] for the 0.8-eV emission. The second level of As_{Ga} is located at $E_v+0.5$ eV. Considering the known Franck-Condon shift[11] of 0.11 eV for the first level of As_{Ga}, it is unlikely that the 0.8-eV emission originates from the conduction band to the second level of As_{Ga}. The As_{Ga}-V_{As} center was assigned[21] for the 0.8-eV emission in view of the peak intensity of the 0.8-eV emission and the MBE growth condition. It is difficult to think of V_{As} in the present As-rich low-temperature GaAs. Contrary to the above model, our model based on the identification of the (As_i-V_{Ga}) for the 1.467-eV band exciton, the same heat-treatment effect of the 1.467-eV

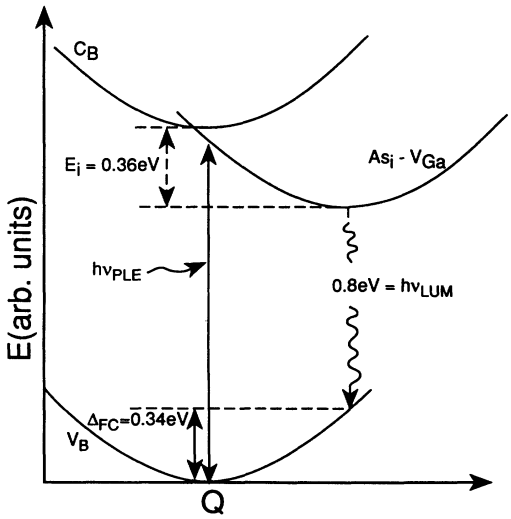

FIG. 7. Configuration coordinate diagram of the As_i-V_{Ga} pair center responsible for the 0.8-eV emission.

exciton and the 0.8-eV emission, and the explanation of the M shape of the 0.8 eV in a LEC wafer can be considered to be a real model for the 0.8-eV emission.

IV. CONCLUSION

We showed that deep-center photoluminescence from MBE layers grown at 200–400 °C strongly depends on the growth temperature and $[As_4]/[Ga]$ BEP ratio. The 200 °C grown layers show the 1.1-eV emission and the 0.68-$EL2$ emission with the relative intensities depending on the $[As_4]/[Ga]$ ratio. The 250 and 300 °C grown layers mainly show the $EL2$ 0.68-eV emission. The substrates were removed from the epitaxial layers in order to confirm the presence of the 0.68-eV $EL2$ emission in the low-temperature-grown layers since the PL of undoped semi-insulating LEC substrates provides a strong 0.68-eV $EL2$ emission. The layers grown at 325 °C and above are dominated by the 0.75- to 0.81-eV emission (designated as the "0.8"-eV emission). Temperature-dependent measurements of the 0.8-eV emission were made. The Huang and Rhys constant (S) and Franck-Condon shift (Δ_{FC}) were determined to be $S=8.9$ and $\Delta_{FC}=0.344$ eV, respectively. The thermal ionization of $E_i=0.36$ eV was determined for the level responsible for the 0.8-eV emission. Measurements of the 0.8-eV and the ~ 1.47-eV bound exciton in heat-treated samples show that the exciton is bound to the deep center responsible for the 0.8-eV emission. Thus, we attribute the 0.8-eV emission to the transition from the As_i-V_{Ga} level to the band edge. On the basis of previous information on $EL6$, we have discussed the possibility of identifying the As_i-V_{Ga} with $EL6$.

ACKNOWLEDGMENTS

We gratefully acknowledge the technical assistance of W. Rice, J. E. Ehret, and E. Taylor. The work of P.W.Y. was performed at Wright Laboratory, Solid State Electronics Directorate (WL/EL), Wright-Patterson Air Force Base under Contract No. F33615-91-C-1765. This work was partially funded by the Air Force Office of Scientific Research.

[1]F. W. Smith, A. R. Calawa, C. L. Chen, M. J. Manfra, and L. J. Mahoney, IEEE Trans. Electron Device Lett. **9**, 77 (1988).
[2]S. Y. Chou, Y. Liu, W. Khalil, T. Y. Hsiang, and S. Alexander, Appl. Phys. Lett. **61**, 819 (1992).
[3]M. Kaminska, Z. Lilental-Weber, E. R. Weber, T. George, J. B. Kortright, F. W. Smith, B.-Y. Tsaur, and A. R. Calawa, Appl. Phys. Lett. **54**, 1881 (1989).
[4]M. R. Melloch, N. Otsuka, J. M. Woodall, and A. C. Warren, Appl. Phys. Lett. **57**, 153 (1990).
[5]A. C. Warren, J. M. Woodall, J. L. Freeoff, D. Grischkowski, D. T. McIntarff, M. R. Melloch, and N. Otsuka, Appl. Phys. Lett. **57**, 1331 (1990).
[6]D. C. Look, D. C. Walters, M. O. Manasreh, J. R. Sizelove, C. E. Stutz, and K. R. Evans, Phys. Rev. B **42**, 3578 (1990).
[7]R. E. Viturro, M. R. Melloch, and J. M. Woodall, Appl. Phys. Lett. **60**, 3007 (1992).
[8]I. Ohbu, M. Takahama, and H. Kimura, Appl. Phys. Lett. **61**, 1679 (1992).
[9]P. W. Yu, D. C. Reynolds, and C. E. Stutz, Appl. Phys. Lett. **61**, 1432 (1992).
[10]P. W. Yu, D. N. Talwar, and C. E. Stutz, Appl. Phys. Lett. **62**, 2608 (1993).
[11]P. W. Yu, Solid State Commun. **43**, 953 (1982).
[12]P. W. Yu, Phys. Rev. B **31**, 8259 (1985).
[13]C. A. Warwick and G. T. Brown, Appl. Phys. Lett. **46**, 574 (1985).
[14]P. W. Yu, D. E. Holmes, and R. T. Chen, in *Gallium Arsenide and Related Compounds 1981,* edited by T. Sugano, IOP Conf. Proc. No. 63 (Institute of Physics, Bristol, 1982) p. 209.
[15]M. Tajima, Jpn. J. Appl. Phys. **21**, L227 (1982).
[16]T. Kikuta, T. Terashina, and K. Ishida, Jpn. J. Appl. Phys. **22**, L409 (1983).
[17]P. W. Yu, Phys. Rev. B **29**, 2283 (1984).
[18]J. Windscheif, H. Ennen, U. Kaufmann, J. Schneider, and T. Kimura, Appl. Phys. A **30**, 47 (1983).
[19]P. W. Yu, in *Proceedings of the 17th International Conference on the Physics of Semiconductors, 1985,* edited by J. D. Chadi and W. W. Harrison (Springer-Verlag, New York, 1985), p. 747.
[20]N. M. Haegel and Y. J. Kao, Appl. Phys. A **50**, 249 (1990).
[21]M. Shinohara, J. Appl. Phys. **61**, 365 (1987).
[22]Details of PLE measurements will be published elsewhere.
[23]J. A. Rossi, C. M. Wolfe, G. E. Stillman, and J. O. Dimmock, Solid State Commun. **8**, 2021 (1970).
[24]R. Dingle, C. Wiesbuch, H. L. Stoïrmer, H. Mockoc, and A. Y. Cho, Appl. Phys. Lett. **40**, 507 (1982).
[25]G. M. Martin, E. Estéve, P. Langlade, and S. Makram-Ebeid, J. Appl. Phys. **56**, 2655 (1984).
[26]J. Samitier, J. R. Morante, L. Girodet, and S. Gourrier, Appl. Phys. Lett. **48**, 1138 (1986).
[27]D. J. Chadi and K. J. Chang, Phys. Rev. Lett. **60**, 2187 (1988); J. Dabrowski and M. Scheffler, *ibid.* **60**, 2183 (1988).
[28]M. Tajima and Y. Okada, Physica **116B**, 404 (1983).
[29]P. W. Yu and C. E. Stutz, J. Electron. Mater. **22**, 1441 (1993).
[30]K. Leo, W. W. Rühle, and N. M. Haegel, J. Appl. Phys. **62**, 3055 (1987).
[31]D. J. Stirland, I. Grant, M. R. Brozel, and R. M. Ware, in IOP Conf. Proc. No. 67 (IOP, Bristol, 1983), p. 285.
[32]T. Figielski, T. Wonsinski, and A. Mokasa, Phys. Status Solidi A **131**, 369 (1992).